Size effects of small-scale beams in bending addressed with a strain-difference based nonlocal elasticity theory

P. Fuschi[a], A.A. Pisano[a], C. Polizzotto[b]

[a] *University Mediterranea of Reggio Calabria, Dipartimento Patrimonio Architettura Urbanistica, Via Melissari, 89124 Reggio Calabria, Italy*
[b] *University of Palermo, Dipartimento di Ingegneria Civile, Ambientale, Aerospaziale, dei Materiali, Viale delle Scienze, 90128 Palermo, Italy*

Abstract

A strain-difference based nonlocal elasticity model devised by the authors elsewhere (Polizzotto et al., Int. J. Solids Struct. 25 (2006) 308–333) is applied to small-scale homogeneous beam models in bending under static loads in the purpose to describe the inherent size effects. With this theory —belonging to the strain-integral nonlocal model family, but exempt from anomalies typical of the Eringen nonlocal theory— the relevant beam problem is reduced to a set of three mutually independent Fredholm integral equations of the second kind (each independent of the beam's ordinary boundary conditions, only one depends on the given load), which can be routinely solved numerically. Applications to five cases of beam samples (usually addressed in the literature) are performed, the obtained results are graphically illustrated and compared with analogous results from the literature. Size effects of *stiffening* type are found for all beam samples, in agreement with the analogous results obtained with the well-known and widely accepted strain gradient elasticity model. Analogous size effects are expected to be predicted for other multi-dimensional structures, all of which seems to confirm the *smaller-is-stiffer* phenomenon.

Keywords: Beam theory, Nonlocal elasticity, Beam structures, Size effects

*corresponding author: aurora.pisano@unirc.it (Aurora Angela Pisano)

Preprint submitted to International Journal of Mechanical Sciences December 12, 2018

1. Introduction

The behavior of beam structures at micro- and nano-scales has been widely studied within the nonlocal (stress-gradient) elasticity theory advanced by Eringen (1983, 2002). This theory is characterized by a stress-strain relation of integral type, in which the stress (conventionally called "nonlocal") measured at a point is expressed as a weighted mean value in terms of the strain (conventionally called "local") measured at all points within the domain occupied by the material. Additionally, the kernel function of this integral relationship (through which a length scale parameter for the underlined microstructure is carried in) is taken coincident with the Green function of a Helmholtz differential equation in the nonlocal stress, such that the solution of the integral equation may be equivalently obtained as the solution of the differential equation. Eringen (1983, 2002) provided mathematical forms of the kernel function for one-, two- and three-dimensional domains and probed them by comparisons of the dispersion curves of Rayleigh surface waves and of screw dislocations obtained by means of the proposed nonlocal theory with the analogous curves obtained by means of atomistic lattice dynamics (Wang and Hu, 2005; Zhang et al., 2006; Heireche et al., 2008; Khorshidi and Fallah, 2016; Shaat and Abdelkefi, 2017; Patra et al., 2018).

The Eringen nonlocal elasticity described above, here (as often in the literature) referred to as the nonlocal "differential", or "stress-gradient", model, constitutes an appealing conceptual framework for the study of the size effects exhibited by small scale structures due to the inhomogeneities and defects of the inherent microstructure. There exists a huge literature in which this theory is applied to beam and plate models simulating sensors and actuators within modern micro- and nano-technologies. Here we just mention a few representative works as (Peddieson et al., 2003; Sudak, 2003; Reddy, 2007; Gibson et al., 2007; Kumar et al., 2008; Pin Lu et al., 2007; Aydogdu, 2009; Eltaher et al., 2016; Reddy, 2010; Wang and Arash, 2014; Li et al., 2015; Xu et al., 2016; Eptaimeros et al., 2016; Rafii et al., 2016; Faroughi et al., 2017).

Two decades after its birth, the Eringen nonlocal differential elasticity theory was applied by Peddieson et al. (2003) to simple nanobeams in bending simulating sensors and actuators devises within micro- and nano-technologies for which clear predictions of size-dependent effects were expected. It was found that this theory is not able by its own nature to predict size effects in a cantilever beam subjected to point load(s), but it predicts stiffening size effects for the same beam under a uniform load, whereas it in general predicts softening size effects for beams with different constraint conditions. Anomalous results were also found for a beam under free vibration (Lu et al., 2006) and buckling condition (Sudak, 2003), and for a rod in tension (Benvenuti and Simone, 2013).

These anomalies were subsequently addressed by many researchers, who advanced remedies to overcome them. For instance, we recall (Polizzotto, 2001; Pisano and Fuschi, 2003; Benvenuti and Simone, 2013; Khodabakhshi and Reddy, 2015; Wang et al., 2016), where a two-phase local/nonlocal model is used in place of the Eringen's fully nonlocal one; (Challamel et al., 2016), where the Eringen's fully nonlocal model is used, but the solution is searched out of the usual displacement continuity framework; (Challamel and Wang, 2008; Lim et al., 2015; Xu et al., 2017a,b), where a hybrid model is used, which is formed up by the Eringen's nonlocal stress-gradient model coupled with a strain gradient one, such that the material behavior is governed by two different types of length scale parameters; (Fernández-Sáez et al., 2016; Wang et al., 2016), where the nonlocal bending moment solution is found as a solution of the Helmholtz differential equation accompanied by special boundary conditions (known from integral equation theory, see Tricomi (1985); Polyanin and Manzhirov (2008)) which in principle guarantee the equivalence between the differential problem and the nonlocal one; (Tuna and Kirca, 2016), where mathematical procedures of integral equation theory are applied to derive "exact" solutions to the Eringen's nonlocal beam problem (indeed a problem known to admit no solution (Romano and Barretta (2016)).

Mention is also given of a research stream within micro/nano-technologies, in which suitable forms of the Eringen nonlocal theory are used to solve nonlinear problems. Within this framework we recall (Vila et al., 2017) in which one-dimensional solids in vibration are addressed, obtained through a continualization procedure from a discrete molecular model undergoing large displacements; (Sahmani and Aghdam, 2017a,b) where the instability of nonlocal nano-shells is addressed; (Lu et al., 2017) where a nonlocal strain gradient theory is used to study nano-beams in vibration; (Sahmani et al., 2018a,b) where functional graded nano-beams and nano-plates in bending and vibration are addressed; (Pang et al., 2018) where the vibration of visco-elastic nano-plates with surface stresses are considered; (Pinto and Mordehai, 2018) where combined longitudinal and transverse vibrations of nanowires are studied; (Sahmani et al., 2018c) where the nonlocal strain gradient theory is used to study the instability of functionally graded micro/nano-plates.

Research efforts were spent for the study of the so-called *boundary effects*, which manifest themselves within a boundary layer of a finite domain occupied by a nonlocal material of Eringen type. As a consequence of these effects, the nonlocal stress response to a uniform strain field is not uniform, whereas instead it is expected to be uniform whenever any source of nonlocality does not occur. A discussion on the above boundary effects can be found in (Romano et al., 2017b, 2018).

This latter shortcoming was eliminated within the framework of nonlocal damage theory, first by Pijaudier-Cabot and Bažant (1987) who adopted a suitably rescaled, but non-symmetric, kernel; then by Borino et al. (2002, 2003), who proposed a differently modified symmetric kernel. Within the framework of nonlocal elasticity, Polizzotto (2002); Polizzotto et al. (2004) advanced a strain-difference based model; this happens to be equivalent to the latter referenced model, but it was independently conceived as a nonlocal counterpart of a strain gradient model whereby the stress response proves to be uniform as soon as the source strain field is uniform. The latter requirement for the stress response was subsequently incorporated into a more general *locality recovery condition* in (Polizzotto et al., 2006) (see Subsection 2.2).

A deeper insight on the Eringen nonlocal differential theory was given by Romano et al. (2017a), who discussed the basic role there played by the mentioned special boundary conditions. Romano and Barretta (2017a,b); Romano et al. (2017b) proposed a "stress-driven" nonlocal model featured by an integral equation formally like the Eringen's one, but with the stress and strain state variables having interchanged roles. Extensions of this theory to mixture models, functionally graded materials and multi-dimensional domains were reported and discussed in Romano et al. (2018); Barretta et al. (2018). Indeed, the stress-driven nonlocal theory by Romano and co-workers seems to have given a clear understanding about the limits of validity of the Eringen's nonlocal theory.

It emerges from the above that the Eringen nonlocal differential theory seems to be unable by its own nature to predict size effects of structures without the mentioned drawbacks, nor to predict size effects agreeing with those (in general of stiffening type) predicted by strain gradient elasticity theory (Mindlin, 1965; Mindlin and Eshel, 1968; Gao and Park, 2007) and detected by laboratory experiments (Fleck et al., 1994; Lam et al., 2003; Sun et al., 2008; Zhao et al., 2009; Abazari et al., 2015; Li et al., 2018).

Therefore, it seems to be useful to investigate on the possibility to replace the Eringen's nonlocal model with another one also belonging to the strain-integral model family, but *exempt from all the previously described drawbacks and capable to predict stiffening size effects like the strain gradient model*. The improved constitutive models, previously mentioned as remedies to the drawbacks of the Eringen nonlocal model, comply each only in part with the above requirement; for instance, the two-phase local/nonlocal model, originally proposed by Eringen himself (Eringen, 1972, 1987), does lead to a Fredholm integral equation of the second kind, but it arrives at stresses not satisfying the locality recovery condition.

In the present paper we will show that, for the analysis of (stiffening) size effects in small-scale structures, the so-called *strain-difference based nonlocal elasticity* model cast in the form envisioned in (Polizzotto et al., 2006) can be usefully applied in competition to the strain gradient model. As better explained subsequently, this nonlocal model is featured by properties not shared by the Eringen one, that is:

1. It obeys the locality recovery condition, which implies that the classical Hooke law is recovered in the presence of a *uniform* strain field, no matter the value of the length scale parameter.
2. It leads to a Fredholm integral equation of the second kind.

Additionally, like the original Eringen model (Eringen, 1972, 1987), the mentioned strain-difference based model does not require that the kernel function be the Green function of a differential equation.

Since the mentioned strain-difference model incorporates a linearized elasticity theory, only linear problems within statics and dynamics can be addressed with it. Extensions to nonlinear situations are possible in principle, but not available so far. In the present paper only applications to static problems are considered, indeed a framework where the strain-difference based model lends itself to a solution method that may be of interest; vibration and buckling problems will be addressed in the near future. For simplicity, axial displacements and shear deformation with warping of the cross section (Reddy, 2007, 2010; Polizzotto, 2015, 2017) are disregarded, but both of them may be straightforwardly implemented with the present model.

1.1. Outline

The outline of the present paper is as follows. In Section 2, the Eringen nonlocal differential method is discussed to point out, aside its basic appealing conceptual framework, the accompanying drawbacks. A brief account of the remedies proposed in the literature is reported. In Section 3, the strain-difference based nonlocal elasticity model is briefly presented and its one-dimensional version for beam structures in bending is reported for later use. The general beam bending problem is discussed in Section 4, where it is found that the typical beam problem can be reverted to the solution of three mutual independent Fredholm integral equations of the second kind, each being independent of the beam ordinary boundary conditions, while only one of them is affected by the load. Section 5 is devoted to the applications whereby five beam cases usually considered in the literature are addressed and the related results are reported graphically together with analogous results from the literature. Conclusions are drawn in the final Section 6.

1.2. Notation

A standard notation is used throughout. The meaning of particular symbols used on occasion will be given in the text at their first appearance.

2. Some remarks on the Eringen nonlocal elasticity model

In this section, some useful remarks on the Eringen nonlocal elasticity model (Eringen, 1972, 1983, 1987, 2002) are reported. For this purpose, reference is made to a simple Euler–Bernoulli beam of length L, referred to orthogonal co-ordinates (x, y, z), with x coinciding with the beam axis, z along the beam height, y in the width direction. The Hooke stress reads as $\sigma = E\varepsilon$, where $\sigma = \sigma_{xx}$, $\varepsilon = \varepsilon_{xx}$, whereas E is the Young modulus. The plane (x, z) coincides with the bending plane, the z axis is a principal inertia axis.

2.1. Equivalence to a Fredholm integral equation of first kind

Written in terms of bending moment M and bending curvature χ, the stress-strain relation of the Eringen nonlocal model for a homogeneous beam reads as

$$M(x) = EI \int_0^L g(x, \bar{x}) \chi(\bar{x}) \, \mathrm{d}\bar{x} \tag{1}$$

where I is the second area moment of the cross section. For a one-dimensional domain, the kernel function $g(x, \bar{x})$ was suggested by Eringen (Eringen, 1983, 2002) in the form of a bi-exponential function, that is,

$$g(x, \bar{x}) = \frac{1}{2\ell} \exp\left(-\frac{r}{\ell}\right) \tag{2}$$

where $r := |\bar{x} - x|$, and $\ell > 0$ is a length scale parameter. The kernel g proves to be the Green function of the Helmholtz equation

$$M(x) - \ell^2 M''(x) = EI\chi(x) \tag{3}$$

and it moreover satisfies the normalization condition

$$\int_{-\infty}^{+\infty} g(x, \bar{x}) \, \mathrm{d}\bar{x} = 1 \qquad \forall x \tag{4}$$

The latter equality implies that, at the limit for $\ell \to 0^+$, the kernel $g \to \delta_D$ (Dirac delta), hence (1) recovers its classical form, $M = EI\chi$, correspondingly.

A serious drawback of (1) is that, considering $M(x)$ as a specified field, (1) constitutes a Fredholm integral equation of the first kind for the unknown curvature $\chi(x)$, indeed, an integral equation known to may lead to not well-posed boundary-value problems with multiple solutions, or even no solution at all (Tricomi, 1985; Polyanin and Manzhirov, 2008). Additionally, in order that the solution of the Helmholtz equation (3) be also a solution of the integral equation (1), it is necessary that the given function $M(x)$ satisfies the special boundary conditions (Tricomi, 1985; Polyanin and Manzhirov, 2008):

$$\left.\begin{aligned} -M'(0) + \tfrac{1}{\ell} M(0) = 0 \\ M'(L) + \tfrac{1}{\ell} M(L) = 0 \end{aligned}\right\} \tag{5}$$

But, as already pointed out by Romano et al. (2017a), the boundary conditions (5) may likely be in so strong contrast with the ordinary (static) boundary conditions of the beam problem such as to impede a solution of the nonlocal integral problem to exist.

Often in the literature (see e.g. Peddieson et al. (2003); Reddy (2007); Challamel and Wang (2008); Polizzotto (2014)) the nonlocal beam problem is addressed through only the differential equation (3) combined with the equilibrium equation $M''(x) = -p(x)$ and the ordinary boundary conditions, by which a *unique* solution can be obtained. This solution may coincide with the classical counterpart (like in the case of a cantilever beam under a point load), but in general it is *not* a solution of the Eringen nonlocal integral problem, which latter has *no solution* as long as the special boundary conditions (5) cannot be satisfied (Romano et al., 2017a).

As reported in the preceding section, a remedy to this drawback consists in replacing the Eringen fully nonlocal model with a two-phase local/nonlocal one with specified volume fractions, which leads to a Fredholm integral equation of the second kind. However, as mentioned previously (and better explained in next subsection), the latter model does not comply with the locality recovery condition.

2.2. The locality recovery condition

The "locality recovery condition" recalled here was first advanced in (Polizzotto et al., 2006) with reference to nonlocal elastic materials, then it was extended to plasticity (Polizzotto, 2007) and generalized continua (Polizzotto and Pisano, 2012). To the readers' benefit, here we briefly recall the inherent essential concepts.

The locality recovery condition constitutes a thermodynamic requisite of a nonsimple material which under any uniform strain mechanism behaves like a simple material, featured by a Helmholtz free energy independent of the inherent length-scale parameter. In order that the latter requisite be satisfied, it is required that the *Energy Residual* (ER) (that is, the energy density transmitted to the generic particle within the body from all other particles therein as a consequence of the non-locality effects) *has to vanish identically under any uniform strain field.*

The necessity of a locality recovery condition serves to guarantee that the constitutive model be able to capture a basic behavioral micro-scale phenomenon whereby *no size effects occur under uniform strain.* For a strain gradient material, in which the free energy is a function of the strain and the strain gradient(s), the locality recovery condition is automatically satisfied due to the correspondingly vanishing of the strain gradient(s).

Instead, for a nonlocal strain-integral (or strain-driven) model, in which the free energy depends on the average of the strain over the whole domain and is thus influenced by the boundary effects, the locality recovery condition is not automatically satisfied, hence it needs to be enforced by eliminating the mentioned boundary effects.

There is not a general consensus in the literature about the necessity of a locality recovery condition. Nonlocal models not obeying the locality recovery condition (like e.g. the two-phase local/nonlocal models) are in fact often used in research, but obviously one has to be aware that then some sort of size effects remain active under any uniform strain mechanism. Nevertheless, in the present paper the mentioned condition is considered as a basic requisite for a nonlocal material model suitable to size effects analysis problems.

In the case of a *homogeneous nonlocal elastic material* the locality recovery condition takes on the simpler form of *local stress recovery condition*, that is, the nonlocal stress response is uniform whenever the imposed local strain is uniform.

For a nonlocal beam model under a uniform curvature, say $\chi = \chi_0 =$ constant, (1) gives a bending moment as

$$M(x) = \gamma(x) EI \chi_0 \tag{6}$$

where $\gamma(x)$ is a weight function defined as

$$\gamma(x) := \int_0^L g(x, \bar{x}) \, \mathrm{d}\bar{x} \tag{7}$$

Indeed, Eq. (1) gives a bending moment response to a given uniform imposed curvature, which is *non-uniform and affected by size effects* through the ℓ parameter (carried in by the kernel function incorporated into the function γ); in other words, (1) does not obey the locality recovery condition.

A remedy to this drawback is obtained by rewriting (1) in the form

$$M(x) = EI\chi(x) + \int_0^L g(x, \bar{x}) EI[\chi(\bar{x}) - \chi(x)] \, \mathrm{d}\bar{x} \tag{8}$$

or equivalently

$$M(x) = [1 - \gamma(x)]EI\chi(x) + \int_0^L g(x,\bar{x})EI\chi(\bar{x})\,\mathrm{d}\bar{x} \tag{9}$$

The latter equations describe a mixed local/nonlocal model which obviously satisfies the locality recovery condition and concomitantly makes the boundary effects be entirely compensated. Both Eqs. (8) and (9) were proposed in (Polizzotto, 2002; Polizzotto et al., 2004). As previously recalled in the Introduction, an equation substantially equivalent to (9) was independently contributed by (Borino et al., 2002, 2003).

2.3. Incomplete redistribution of the source local bending moment

The Eringen nonlocal model (1) can be interpreted as an analytical tool by which the source local bending moment $M^{\mathrm{lc}}(x) := EI\chi(x)$ at x is redistributed within the beam length, giving rise to a smooth long distance specific bending moment $\mu(\bar{x},x) := g(\bar{x},x)M^{\mathrm{lc}}(x)$ at the generic point $\bar{x}$ within $(0,L)$; (the dimension of μ is a force).

A good physically consistent property of the nonlocal beam may be that the totality of long distance bending moments $\mu(\bar{x},x)$ within $(0,L)$ be equal to $M^{\mathrm{lc}}(x)$ at every x in $(0,L)$. Indeed, for a beam enjoying this property (here qualified as *stress saving beam*), the inherent non-locality consists in a complete redistribution of the source local bending moment $M^{\mathrm{lc}}(x)$ at every point of the beam, without losses, nor additions.

This desirable property is naturally satisfied in the case of unbounded domain, but it is not in the opposite case, since in fact the related resultant long distance specific bending moment proves to be

$$\int_0^L \mu(\bar{x},x)\,\mathrm{d}\bar{x} = \gamma(x)M^{\mathrm{lc}}(x) \tag{10}$$

Since $0 < \gamma(x) \leq 1\ \forall x \in (0,L)$, it results that, at every point x where $\gamma(x) < 1$, *only the fraction* $\gamma(x)M^{\mathrm{lc}}(x)$ *of the source local bending moment is redistributed while the remaining part, amounting to* $[1-\gamma(x)]M^{\mathrm{lc}}(x)$*, is just thrown away*, with consequent *loss in stiffness*. This behavior of the Eringen nonlocal model is likely the very reason why this model predicts softening size effects in the majority of cases; it constitutes a drawback that manifests itself through the previously mentioned boundary effects.

A remedy to this drawback is to express the bending moment $M(x)$ as the sum of the non-redistributed part of the local bending moment $M^{\mathrm{lc}}(x)$, along with the total long distance bending moment arriving at x from all other points of the beam, that is,

$$M(x) = \underbrace{[1-\gamma(x)]EI\chi(x)}_{\text{non-redistributed local bending moment}} + \underbrace{\int_0^L g(x,\bar{x})EI\chi(\bar{x})\,\mathrm{d}\bar{x}}_{\text{total long distance bending moment}} \tag{11}$$

which happens to coincide with (9).

Eq. (11) was the source of inspiration for the strain-difference nonlocal model advanced in (Polizzotto et al., 2004) and then of the improved one in (Polizzotto et al., 2006).

In closing this section, we state that the strain-difference based nonlocal model proposed by Polizzotto et al. (2006) is capable to overcome all the above drawbacks. Indeed, this model is stress-saving (i.e. the stress redistribution process is complete everywhere within any body of finite extension). Furthermore, it leads to a Fredholm integral equation of the second kind, complies with the locality recovery condition and generally predicts stiffening size effects.

3. The strain-difference based nonlocal elasticity model

In this section, the strain-difference based nonlocal elasticity model in the form advanced in (Polizzotto et al., 2006) is briefly described for later use.

3.1. General

The strain-difference based nonlocal model is a phenomenological model capable to cope with inhomogeneities of both the moduli and the internal length scale. It is thermodynamically consistent, as it is centered on a Helmholtz free energy, say ψ, which for a three-dimensional body is cast in a compact form as [1]

[1] In the case of homogeneous materials, an alternative form of ψ of (12) may be $\psi = 0.5\,\boldsymbol{\varepsilon} : \mathbf{C} : \boldsymbol{\varepsilon} + 0.5\,\boldsymbol{\varepsilon} : \alpha\,\mathbf{C} : \mathcal{R}(\boldsymbol{\varepsilon})$, which would lead to the simpler stress-strain equation

$$\psi = \frac{1}{2}\,\boldsymbol{\varepsilon} : \mathbf{C} : \boldsymbol{\varepsilon} + \frac{1}{2}\,\mathcal{R}(\mathcal{D}\boldsymbol{\varepsilon}) : (\alpha\mathbf{C}) : \mathcal{R}(\mathcal{D}\boldsymbol{\varepsilon}) \tag{12}$$

where $\mathbf{C} = \mathbf{C}(\mathbf{x})$ is the standard elastic moduli tensor of anisotropic elasticity, α is a non-negative material constant. The symbol $\mathcal{D}\boldsymbol{\varepsilon}$ denotes the strain difference at points $\mathbf{x}, \bar{\mathbf{x}}$, that is,

$$\mathcal{D}\boldsymbol{\varepsilon}(\mathbf{x}, \bar{\mathbf{x}}) := \boldsymbol{\varepsilon}(\bar{\mathbf{x}}) - \boldsymbol{\varepsilon}(\mathbf{x}) \quad \forall(\mathbf{x}, \bar{\mathbf{x}}) \in V \tag{13}$$

whereas the symbol $\mathcal{R}(\mathcal{D}\boldsymbol{\varepsilon})$ is defined as

$$\mathcal{R}(\mathcal{D}\boldsymbol{\varepsilon})(\mathbf{x}) := \int_V g(\mathbf{x}, \bar{\mathbf{x}})\underbrace{[\boldsymbol{\varepsilon}(\bar{\mathbf{x}}) - \boldsymbol{\varepsilon}(\mathbf{x})]}_{\mathcal{D}\boldsymbol{\varepsilon}(\mathbf{x},\bar{\mathbf{x}})}\,\mathrm{d}V(\bar{x}) \tag{14}$$

Here, the (symmetric) kernel $g(\mathbf{x}, \bar{\mathbf{x}})$ is a two-point attenuation function similar to the analogous kernel presented in Section 2; it satisfies the normalization condition (4), but is not necessarily the Green function of a differential equation.

As reported in (Polizzotto et al., 2006), the attenuation function $g(x, \bar{x})$ is taken in the form

$$g(x, \bar{x}) = \bar{g}\Big(-\frac{r_{\mathrm{eq}}}{\ell_0}\Big) \tag{15}$$

where ℓ_0 is the reference length scale parameter taken equal to the largest value of the space-variable length scale parameter $\ell(\mathbf{x})$, whereas r_{eq} denotes the *equivalent distance* defined as

$$r_{\mathrm{eq}} := r + r^* \tag{16}$$

Here, r is the so-called *geodetical distance*, meant as the length of the shortest path between any two points of a domain without intersecting its boundary. For a non-convex domain (due e.g. to holes or cracks) it is $r \geq |\bar{\mathbf{x}} - \mathbf{x}|$, but $r = |\bar{\mathbf{x}} - \mathbf{x}|$ for a convex one. The quantity r^* constitutes a fictitious (non-negative) distance which accounts the additional attenuation effects due to the material inhomogeneities through the stiffness tensor $\mathbf{C}(\mathbf{x})$ and the length scale parameter $\ell(\mathbf{x})$. Motivations to consider additional

$\boldsymbol{\sigma} = \mathbf{C} : [\boldsymbol{\varepsilon} + \alpha\mathcal{R}(\boldsymbol{\varepsilon})]$ often used in the literature, but it does not satisfy the locality recovery condition since, for $\boldsymbol{\varepsilon} = \bar{\boldsymbol{\varepsilon}} =$ const., it is $\boldsymbol{\sigma} = \mathbf{C} : \bar{\boldsymbol{\varepsilon}}[1 + \alpha\gamma(\mathbf{x})]$.

attenuation effects in the presence of inhomogeneities are given in (Polizzotto et al., 2006). In the present work, however, we consider convex domains and homogeneous materials, hence $r = |\bar{\mathbf{x}} - \mathbf{x}|$, $\ell =$ constant throughout.

$\mathcal{R}(\mathcal{D}\boldsymbol{\varepsilon})$ is the weighted mean value of the strain difference $\mathcal{D}\boldsymbol{\varepsilon}$ around the field point $\mathbf{x} \in V$; it is a measure of the nonlocal part of the strain at $\bar{\mathbf{x}}$. Obviously, was $\boldsymbol{\varepsilon}$ uniform within V, it would be $\mathcal{R}(\mathcal{D}\boldsymbol{\varepsilon}) \equiv \mathbf{0}$, that is, the locality recovery condition is automatically satisfied, like with a strain gradient model.

The energy ψ, a quadratic form of the strain $\boldsymbol{\varepsilon}$ and the nonlocal strain difference $\mathcal{R}(\mathcal{D}\boldsymbol{\varepsilon})$, is the sum of two contributions, one from a local constitutive behavior of unit density, the other from a nonlocal constitutive behavior whose density depends on the α coefficient. On increasing α the relative importance of the local phase with respect to the nonlocal one will decrease; for $\alpha \to \infty$ the model tends to lose the accompanying local phase. Therefore, α also plays the role of phase parameter.

The stress-strain relation is obtained from (12) by writing (Polizzotto et al., 2006):

$$\left.\begin{aligned} \mathbf{t} &= \frac{\partial \psi}{\partial \boldsymbol{\varepsilon}} = \mathbf{C} : \boldsymbol{\varepsilon} \\ \boldsymbol{\tau} &= \frac{\partial \psi}{\partial \mathcal{R}(\mathcal{D}\boldsymbol{\varepsilon})} = \alpha \mathbf{C} : \mathcal{R}(\mathcal{D}\boldsymbol{\varepsilon}) \\ \boldsymbol{\sigma} &= \mathbf{t} + \mathcal{R}(\mathcal{D}\boldsymbol{\tau}) \end{aligned}\right\rangle \tag{17}$$

After some mathematics not reported here for brevity sake (for which we refer to (Polizzotto et al., 2006)), Eq. $(17)_3$ reads either as

$$\boldsymbol{\sigma}(\mathbf{x}) = \mathbf{C}(\mathbf{x}) : \boldsymbol{\varepsilon}(\mathbf{x}) - \alpha \int_V \mathbf{J}(\mathbf{x}, \bar{\mathbf{x}}) : [\boldsymbol{\varepsilon}(\bar{\mathbf{x}}) - \boldsymbol{\varepsilon}(\mathbf{x})] \, \mathrm{d}V(\bar{\mathbf{x}}) \tag{18}$$

or equivalently as

$$\boldsymbol{\sigma}(\mathbf{x}) = \mathbf{C}(\mathbf{x}) : \boldsymbol{\varepsilon}(\mathbf{x}) + \alpha \int_V \mathbf{S}(\mathbf{x}, \bar{\mathbf{x}}) : \boldsymbol{\varepsilon}(\bar{\mathbf{x}}) \, \mathrm{d}V(\bar{\mathbf{x}}) \tag{19}$$

The *nonlocal stiffness tensors* $\mathbf{J}$ and $\mathbf{S}$ are expressed as

$$\left.\begin{aligned}\mathbf{J}(\mathbf{x},\bar{\mathbf{x}}) &:= [\gamma(\mathbf{x})\mathbf{C}(\mathbf{x}) + \gamma(\bar{\mathbf{x}})\mathbf{C}(\bar{\mathbf{x}})]g(\mathbf{x},\bar{\mathbf{x}}) \\ &\qquad - \textstyle\int_V g(\mathbf{x},\boldsymbol{\xi})g(\bar{\mathbf{x}},\boldsymbol{\xi})\mathbf{C}(\boldsymbol{\xi})\,\mathrm{d}V(\boldsymbol{\xi}) \\ \mathbf{S}(\mathbf{x},\bar{\mathbf{x}}) &:= \tfrac{1}{2}\left[\gamma^2(\mathbf{x})\mathbf{C}(\mathbf{x}) + \gamma^2(\bar{\mathbf{x}})\mathbf{C}(\bar{\mathbf{x}})\right]\delta_D(\mathbf{x},\bar{\mathbf{x}}) - \mathbf{J}(\mathbf{x},\bar{\mathbf{x}})\end{aligned}\right\} \tag{20}$$

and satisfy the equalities

$$\left.\begin{aligned}&\textstyle\int_V \mathbf{J}(\mathbf{x},\bar{\mathbf{x}})\,\mathrm{d}V(\bar{\mathbf{x}}) = \gamma^2(\mathbf{x})\mathbf{C}(\mathbf{x}) \\ &\textstyle\int_V \mathbf{S}(\mathbf{x},\bar{\mathbf{x}})\,\mathrm{d}V(\bar{\mathbf{x}}) = \mathbf{0}\end{aligned}\right\} \quad \forall\mathbf{x}\in V \tag{21}$$

3.2. The strain-difference beam model in bending

In the case of homogeneous Euler–Bernoulli beam in bending like the one introduced in Section 2, in which $\varepsilon = \varepsilon_{xx}$ is the only meaningful strain component, the transverse attenuation effects are assumed to be of so modest amplitude such that the kernel g can be considered to be a function of the x co-ordinate only, that is, $g = g(x,\bar{x})$. Then, the stress-strain equation (18) simplifies as follows:

$$\sigma(x,z) = E\varepsilon(x,z) - \alpha E\int_0^L \kappa(x,\bar{x})[\varepsilon(\bar{x},z) - \varepsilon(x,z)]\,\mathrm{d}\bar{x} \tag{22}$$

or, equivalently,

$$\sigma(x,z) = E\,[1 + \alpha\gamma^2(x)]\varepsilon(x,z) - \alpha E\int_0^L \kappa(x,\bar{x})\varepsilon(\bar{x},z)\,\mathrm{d}\bar{x} \tag{23}$$

Here, $\kappa(x,\bar{x})$ (dimensionally an inverse length) is given by

$$\kappa(x,\bar{x}) = \left[\gamma(x) + \gamma(\bar{x})\right]g(x,\bar{x}) - \int_0^L g(x,\xi)g(\bar{x},\xi)\,\mathrm{d}\xi \tag{24}$$

Analogously, the stress-strain relation (19) simplifies as

$$\sigma(x,z) = E\varepsilon(x,z) + \alpha E\int_0^L H(x,\bar{x})\varepsilon(\bar{x},z)\,\mathrm{d}\bar{x} \tag{25}$$

where

$$H(x,\bar{x}) := \frac{1}{2}[\gamma^2(x)+\gamma^2(\bar{x})]\delta_D(\bar{x}-x) - \kappa(x,\bar{x}) \tag{26}$$

The following conditions hold true:

$$\left.\begin{array}{rcl} \int_0^L \kappa(x,\bar{x})\,\mathrm{d}\bar{x} & = & \gamma^2(x) \\ \int_0^L H(x,\bar{x})\,\mathrm{d}\bar{x} & = & 0 \end{array}\right\} \forall x \in (0,L) \tag{27}$$

Next, using (22), denoting by $\chi(x)$ the beam curvature at x and recalling that $\varepsilon(x,z) = z\chi(x)$, the bending moment $M(x) = \int_A z\sigma\,\mathrm{d}A$ takes on the expression

$$\boxed{M(x) = EI\Big\{\big[1+\alpha\gamma^2(x)\big]\chi(x) - \alpha\int_0^L \kappa(x,\bar{x})\chi(\bar{x})\,\mathrm{d}\bar{x}\Big\}} \tag{28}$$

Eq. (28) is the fundamental bending moment/curvature relation featuring the strain-difference based nonlocal model under discussion.

3.3. The weight function $\gamma(x)$

For applications to micro- and nano-beams, it may be useful to construct the weight function $\gamma(x)$ of (7) for the bi-exponential kernel (2). This function is a (non-dimensional) function that varies continuously within $(0,L)$ and is symmetric with respect to middle point $x = L/2$; it provides the *nonlocal strain associated to a (uniform) unit local strain field within the body*. For the bi-exponential kernel function (2), by a simple integration we can obtain the function $\gamma(x)$ as follows:

$$\gamma(\xi,\lambda) = 1 - \frac{1}{2}\Big[\exp\Big(-\frac{\xi}{\lambda}\Big) + \exp\Big(-\frac{1-\xi}{\lambda}\Big)\Big] \tag{29}$$

The dependence of γ on the length scale parameter ℓ is explicitly accounted by considering the ratio $\lambda := \ell/L$ as an argument of γ. The symbol $\xi := x/L$ is the non-dimensional abscissa $(0 \leq \xi \leq 1)$.

Eringen (1983) suggested to set $\ell = e_0 a$, where a denotes a characteristic length of the microstructure (particle spacing, grain size, and the like), whereas e_0 is a (non-dimensional) material constant identified as $e_0 \approx 0.39$.

The function $\gamma(\xi, \lambda)$ is plotted in Figure 1 for different values of $\lambda = 0.01; 0.05; 0.1; 0.2$.

Since $\gamma(\xi, \lambda)$ is non-decreasing for ξ increasing within the interval $(0, 0.5)$ while λ is taken fixed, we can write:

$$\begin{aligned} \min_{\xi \in (0,1)} \gamma(\xi, \lambda) &= \gamma(0, \lambda) = c_1(\lambda) := \frac{1}{2}\Big[1 - \exp\Big(-\frac{1}{\lambda}\Big)\Big] \\ \max_{\xi \in (0,1)} \gamma(\xi, \lambda) &= \gamma(0.5, \lambda) = c_2(\lambda) := 1 - \exp\Big(-\frac{1}{2\lambda}\Big) \end{aligned} \tag{30}$$

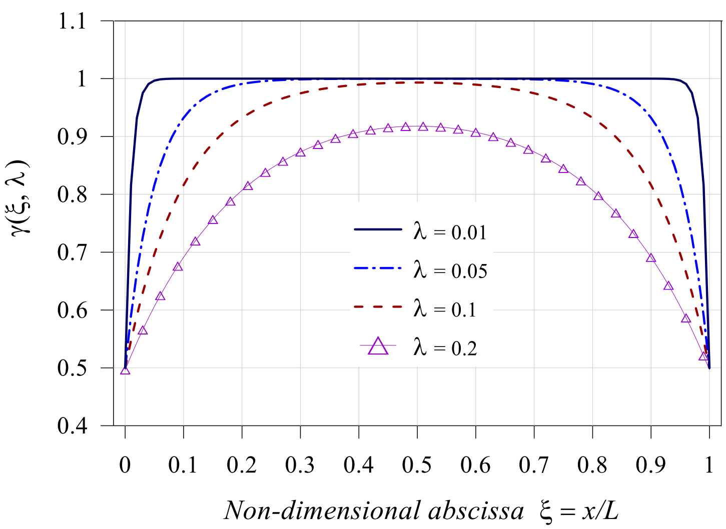

Figure 1: Weight function $\gamma(\xi, \lambda)$ plotted as a function of the non-dimensional abscissa $\xi = x/L$ for $\lambda = 0.01$ (solid line), 0.05 (dash dot line), 0.1 (dashed line) and 0.2 (solid line with triangles).

The bound functions $c_1(\lambda)$ and $c_2(\lambda)$ are plotted in Figure 2, which shows that $c_1(0) = 0.5, c_2(0) = 1$ and that both tend to zero for $\lambda \to \infty$; also, they satisfy the inequalities

$$0 < c_1(\lambda) \leq \frac{1}{2}, \quad 0 < c_2(\lambda) \leq 1, \quad \forall \lambda \geq 0 \tag{31}$$

Since the kernel g is approximately zero at any distance larger than the influence distance, $R = m\ell$, (with $m \approx 6$), then the plots of the functions

$c_1(\lambda)$ and $c_2(\lambda)$ exhibit each an initial constant piece, namely $c_2(\lambda) = 1$ for $0 \leq \lambda \leq \lambda^*$ where $\lambda^* := 1/(2m) \approx 0.0833$, whereas $c_1(\lambda) = 0.5$ for $0 \leq \lambda \leq 2\lambda^*$. Therefore, the bound relation for $\gamma(x, \lambda)$, that is,

$$c_1(\lambda) \leq \gamma(x, \lambda) \leq c_2(\lambda) \quad \forall\ \lambda \tag{32}$$

for λ values smaller than λ^* can be approximated as

$$0.5\ \leq \gamma(x, \lambda) \leq 1 \quad \forall\ \lambda \leq \lambda^* \tag{33}$$

The latter bound relation holds for $L \geq 2R$, that is whenever there exists a core domain of length $L_c := L - 2R = \ell(\frac{1}{\lambda} - \frac{1}{\lambda^*}) > 0$. No core domain can exist whenever $\lambda > \lambda^*$, whereas for $\lambda = \lambda^*$ the core domain exists collapsed at the isolated middle point $x = L/2$.

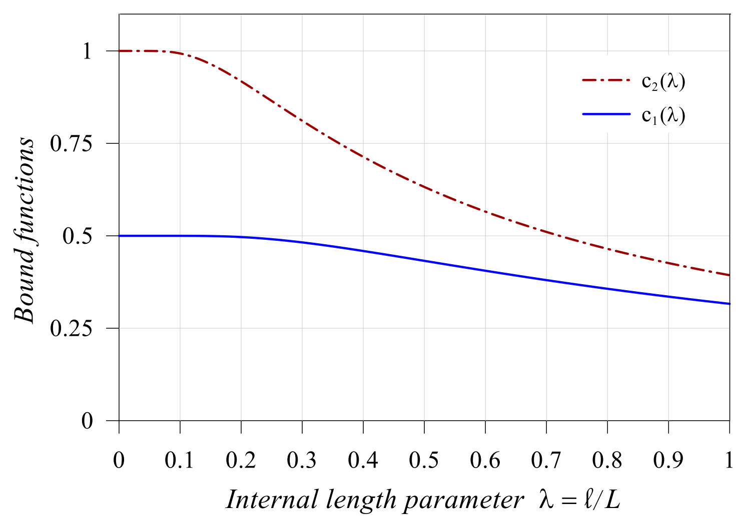

Figure 2: Minimum (c1) and maximum (c2) values of the weight function $\gamma(\xi, \lambda)$ plotted as functions of $\lambda = \ell/L$.

4. The bending beam problem under static loads

Assuming that the beam deforms only in bending without extension, the beam equilibrium equation reads as

$$M''(x) + p(x) = 0 \quad \forall x \in (0, L) \tag{34}$$

where $p(x)$ is the assigned transverse distributed load. By integration of Eq. (34) we can write for convenience:

$$\boxed{M(x) = -f(x) - \frac{EI}{L^2}\big(C_1 x + C_2 L\big)} \tag{35}$$

Here, $f(x)$ is a particular function that satisfies the equation

$$f''(x) = p(x) \qquad \forall x \in (0, L) \tag{36}$$

whereas C_1, C_2 are arbitrary (non-dimensional) constants. Therefore, recalling that $\chi(x) = -w''(x)$, Eq. (28) can be rewritten as

$$\begin{aligned} \big[1 + \alpha\gamma^2(x)\big]\, w''(x) - \alpha \int_0^L \kappa(x, \bar{x}) w''(\bar{x})\, \mathrm{d}\bar{x} = \\ = \frac{1}{EI} f(x) + \frac{1}{L^2}(C_1 x + C_2 L) \end{aligned} \tag{37}$$

Since $1 + \alpha\gamma^2(x) > 0\ \forall x \in (0, L)$, following (Tricomi, 1985), let us posit

$$s(x) := \sqrt{1 + \alpha\gamma^2(x)} \tag{38}$$

and

$$\phi(x) := L s(x) w''(x) \tag{39}$$

Next, solving (39) for $w''(x)$ we can write

$$w''(x) = \frac{1}{L}\frac{\phi(x)}{s(x)} \tag{40}$$

Hence, substituting (40) into (37) leads to the desired Fredholm integral equation of the second kind for the unknown (non-dimensional) function $\phi(x)$, namely,

$$\phi(x) = \alpha \int_0^L K(x, \bar{x}) \phi(\bar{x})\, \mathrm{d}\bar{x} + \frac{L}{EIs(x)} f(x) + C_1 \frac{x}{L} + C_2 \tag{41}$$

where the (symmetric) kernel $K(x, \bar{x})$ is defined as

$$K(x,\bar{x}) := \frac{\kappa(x,\bar{x})}{s(x)s(\bar{x})} \tag{42}$$

The deflection $w(x)$ can be determined by (40) which by integration gives

$$w(x) = L\Psi(x) + C_3 x + C_4 L \tag{43}$$

where C_3 and C_4 are (non-dimensional) arbitrary constants, whereas $\Psi(x)$ is a particular non-dimensional function satisfying the condition

$$L\Psi''(x) = \frac{\phi(x)}{s(x)} \quad \forall x \in (0, L) \tag{44}$$

This $\Psi(x)$ is here chosen in the form

$$\Psi(x) := \frac{1}{L^2}\int_0^x (x-\bar{x})\frac{\phi(\bar{x})}{s(\bar{x})}\,\mathrm{d}\bar{x} \tag{45}$$

The constants C_1, C_2, C_3, C_4 must be determined by the *ordinary* boundary conditions of every specific beam problem, that is, the standard (static and/or kinematic) boundary conditions known from classical beam theories.

4.1. Solution scheme

The integral equation (41), on which the beam problem is centered, can be usefully transformed by splitting the unknown function $\phi(x)$ as

$$\phi(x) = \phi_0(x) + C_1\phi_1(x) + C_2\phi_2(x) \tag{46}$$

Substituting (46) into (41) gives the equality

$$\begin{aligned} &\Big\{\phi_0(x) - \alpha\int_0^L K(x,\bar{x})\phi_0(\bar{x})\,\mathrm{d}\bar{x} - \frac{Lf(x)}{EIs(x)}\Big\} \\ +C_1&\Big\{\phi_1(x) - \alpha\int_0^L K(x,\bar{x})\phi_1(\bar{x})\,\mathrm{d}\bar{x} - \frac{x}{Ls(x)}\Big\} \\ +C_2&\Big\{\phi_2(x) - \alpha\int_0^L K(x,\bar{x})\phi_2(\bar{x})\,\mathrm{d}\bar{x} - \frac{1}{s(x)}\Big\} = 0 \end{aligned} \tag{47}$$

Since the latter equality has to hold for arbitrary values of C_1 and C_2, the following three integral equations must be satisfied, that is,

$$\boxed{\phi_n(x) = \alpha \int_0^L K(x,\bar{x})\phi_n(\bar{x})\,\mathrm{d}\bar{x} + F_n(x), \quad (n=0,1,2)} \tag{48}$$

where it is

$$\left.\begin{array}{rcl} F_0(x) & := & \dfrac{Lf(x)}{EIs(x)} \\ F_1(x) & := & \dfrac{x}{Ls(x)} \\ F_2(x) & := & \dfrac{1}{s(x)} \end{array}\right\rangle \tag{49}$$

Eq. (48) provides a set of three mutually independent Fredholm integral equations of the second kind, all of which hold no matter how the beam ordinary constraints may be; additionally, only the first equation ($n = 0$) depends on the loading conditions.

Next, let (46) be substituted into (45) to obtain

$$\Psi(x) = \Psi_0(x) + C_1\Psi_1(x) + C_2\Psi_2(x) \tag{50}$$

where we have set

$$\boxed{\Psi_n(x) := \frac{1}{L^2}\int_0^x (x-\bar{x})\frac{\phi_n(\bar{x})}{s(\bar{x})}\,\mathrm{d}\bar{x}, \quad (n=0,1,2)} \tag{51}$$

Then, substituting (50) into (43) gives the deflection $w(x)$ cast in the form

$$\boxed{\frac{w(x)}{L} = \Psi_0(x) + C_1\Psi_1(x) + C_2\Psi_2(x) + C_3\frac{x}{L} + C_4} \tag{52}$$

This equation together with (35) constitute a closed-form representation of the solution of the generic beam problem.

The solution for every specific beam problem must be determined taking in account the inherent loading and boundary conditions. This task is achieved in the following section devoted to applications.

5. Applications

Equations (35) and (52) have been applied to a few simple beam cases, that is:

a) Clamped-free beam under a point load P at the free end;

b) Clamped-free beam under uniform distributed load p_0;

c) Pinned-pinned beam under uniform distributed load p_0;

d) Clamped-pinned beam under uniform distributed load p_0;

e) Clamped-clamped beam under uniform distributed load p_0.

For this purpose, the integral equations (48) have been addressed by a routine computational algorithm known from the literature (Press et al., 1997). The resulting deflection curve $w(x)$ and bending moment function $M(x)$ have been computed by (52) and (35) for every case taking $\alpha = 50$, each computation being repeated for λ varying within the interval $(0 \leq \lambda \leq 0.2)$.

The following *ordinary boundary conditions* were adopted in the above computations:

a) Clamped-free beam under end point load:

$$w(0) = w'(0) = M(L) = 0,\ M'(L) = P;$$

b) Clamped-free beam under uniform load:

$$w(0) = w'(0) = M(L) = M'(L) = 0;$$

c) Pinned-pinned beam under uniform load:

$$w(0) = w(L) = M(0) = M(L) = 0;$$

d) Clamped-pinned beam under uniform load:

$$w(0) = w'(0) = w(L) = M(L) = 0;$$

e) Clamped-clamped beam under uniform load:

$$w(0) = w'(0) = w(L) = w'(L) = 0.$$

5.1. *Numerical algorithm to solve the integral equations*

Let the typical integral equation (49) be here reported again in the form

$$\phi(x) = \alpha \int_0^L K(x,y)\phi(y)\,\mathrm{d}y + \psi(x) \tag{53}$$

where $\psi(x)$ identifies itself with $F_n(x), (n = 0, 1, 2)$.

The numerical algorithm used to solve the integral equation (53) is the *Nystrom method* reported in the quoted book (Press et al., 1997), pp. 782–785, by which the desired solution is obtained as the solution of an algebraic linear equation system. The main point consists in choosing a set of quadrature points x_i, $(i = 1, 2, ..., N)$, and a set of weights W_i (Gauss–Legendre quadrature rule). Then, Eq. (53) can be written at every x_i in a discrete form as

$$\phi(x_i) = \alpha \sum_{j=1}^{N} W_j K(x_i, y_j)\phi(y_j) + \psi(x_i) \tag{54}$$

Next, writing ϕ_i for $\phi(x_i)$, $\tilde{K}_{ij}$ for $W_j K(x_i, y_j)$, ψ_i for $\psi(x_i)$, and collecting all of them in vector and matrix forms, we get

$$\left(\mathbf{I} - \alpha\tilde{\mathbf{K}}\right) \cdot \boldsymbol{\phi} = \boldsymbol{\psi} \tag{55}$$

This is a set of N linear equations which generally provides sufficiently accurate values of the unknowns in $\boldsymbol{\phi}$ in terms of the data in $\boldsymbol{\psi}$.

Once the vector $\boldsymbol{\phi}$ is known, the function $\phi(x)$ at the generic point x within $(0, L)$ can be obtained by writing the relation

$$\phi(x) = \alpha \sum_{j=1}^{N} W_j K(x, y_j)\phi_j + \psi(x) \tag{56}$$

Whenever it may be required, the eigenvalues of the matrix $\tilde{\mathbf{K}}$ can be obtained, with the aid of a straightforward symmetrization technique, by addressing the eigenvalue problem

$$\tilde{\mathbf{K}} \cdot \boldsymbol{\phi} = \beta\boldsymbol{\phi}, \quad (\beta = 1/\alpha) \tag{57}$$

According to (Press et al., 1997), the solution of the integral equation with the Nystrom method described above is usually well-conditioned, unless α is very close to an eigenvalue.

5.2. Numerical procedures for the other considered models

For comparison, the analogous plots for other three methods of the literature were also accomplished, of which one is based on the first strain gradient model (Mindlin and Eshel, 1968; Papargyri-Beskou et al., 2003a,b; Polizzotto, 2014) and constitutes the main reference for the present work; another is based on the stress-driven nonlocal model with a bi-exponential kernel (Romano and Barretta, 2017a,b), which is chosen for its similarities with the strain gradient model.[2] The third method is the Eringen nonlocal differential method (Eringen, 1983; Peddieson et al., 2003). The following procedures were adopted to address these comparison models.

(1) *Strain gradient model*

The strain gradient beams were addressed by solving the differential equation (Papargyri-Beskou et al., 2003a,b; Polizzotto, 2014)

$$\Big(w(x) - \ell^2 w''(x)\Big)'''' = \frac{p(x)}{EI} \tag{58}$$

This equation is associated with the ordinary boundary conditions listed above, [3] along with the *higher order* boundary conditions whereby *either the bending curvature* $\chi = -w''$*, or the higher order bending moment* $M^{(1)} = \ell^2 EI\chi' = -\ell^2 EIw'''$*, is specified at the beam ends* (Polizzotto, 2014). This implies that, at each beam end, the rotation and the curvature are allowed to be both fixed, or both free, or even one fixed and the other free, according to the actual constraint conditions.

Among several possible choices for the higher order boundary conditions, we *assumed that the curvature is fixed or free according to whether*

[2]The strain gradient model and the nonlocal stress-driven one are founded on different theoretical bases, but in the case under consideration they are strictly related to a same Helmholtz differential equation, i.e. $M = EI(\chi - \ell\chi'')$. This implies that they share a same governing differential equation, i.e. $(w(x) - \ell^2 w''(x))'''' = p/EI$, and are different from each other only for the respective nonstandard boundary conditions. For this reason the stress-driven nonlocal model has been considered suitable for comparisons with the strain gradient model.

[3]Though in the case of multi-dimensional domain the traction (natural) boundary conditions are different for simple and strain gradient materials, they instead are coincident with each other for one-dimensional domains as in the case under discussion (Polizzotto, 2014).

the rotation is fixed or free, respectively. More precisely, the higher order boundary conditions used to address the beam cases listed above are as follows:

$$\left.\begin{array}{ll} w''(0) = w'''(L) = 0 & \text{for cases a), b), d)} \\ w'''(0) = w'''(L) = 0 & \text{for case c)} \\ w''(0) = w''(L) = 0 & \text{for case e)} \end{array}\right\} \tag{59}$$

(2) *Stress-driven nonlocal model*

The solutions for the stress-driven nonlocal beams were taken from (Barretta et al., 2018), where functionally graded materials are addressed. A comparison of the results of the latter paper with those of the present homogeneous beam model is possible since in (Barretta et al., 2018) the effective Young modulus I_E is constant along the beam axis and its specific influence disappears from the dimensionless quantities therein adopted in equation (91). The solution equations (33), (55), (66), (80) and the numerical data of the tables reported in (Barretta et al., 2018) (with $I_E = EI$) were directly exploited to derive the inherent representative curves. Suitable checks were executed to verify that we were able to exactly reproduce the numerical data collected in the tables reported in (Barretta et al., 2018) by the use of the accompanying closed-form solutions.

A main difficulty for the planned comparison arises from the α coefficient appearing in both models with the role of phase parameter, but with different meanings (in (Barretta et al., 2018): $\alpha = 0 \rightarrow$ fully nonlocal; $\alpha = 1 \rightarrow$ fully local; in the present work: $\alpha = 0 \rightarrow$ fully local; $\alpha \rightarrow \infty, \rightarrow$ fully nonlocal). Additionally, whereas in (Barretta et al., 2018) the kernel just identifies itself with the bi-exponential function, instead in the present work the kernel incorporates squared forms of the latter function, which implies that, at parity of local source strain, the attenuation effects are in some way more pronounced with respect to the former model. Within the planned comparison, this phenomenon may be heuristically accounted by considering as a realistic phase parameter of the present model the quantity $\sqrt{\alpha}$.

Therefore, looking at equation (31) of (Barretta et al., 2018) and Eq. (25) of the present work, a relation between the respective phase parameters may be attempted by writing the equation

$$\sqrt{\alpha_F} : 1 = (1 - \alpha_B) : \alpha_B \tag{60}$$

Here, the subscripts appended to α serve to distinguish the α coefficient of (Barretta et al., 2018) (α_B) from the present one (α_F). From (55) we get

$$\alpha_B = \frac{1}{1 + \sqrt{\alpha_F}} \tag{61}$$

For $\alpha_F = 50$, the latter relation gives $\alpha_B \approx 0.124$. The value $\alpha_B = 0.1$ was used for the computation of the solutions given by (Barretta et al., 2018), which amounts to considering a mixture model with a density of 90 % of the nonlocal phase. [4]

(3) *Eringen's nonlocal model*

The solutions pertaining to the Eringen nonlocal model were taken from (Peddieson et al., 2003), except for the doubly clamped beam not reported in the latter quoted paper, but addressed in (Barretta and Marotti de Sciarra, 2015) and worked out by the authors with the Eringen's method.

It may be useful to note that the doubly clamped Eringen nonlocal beam mentioned above does not exhibit size effects on the deformation, but it does on the bending moment $M(x)$. This is shown in Figure 3, where the $M(x)$ diagram shifts upward on increasing λ (in such a way that the maximum bending moment $M(L/2)$ goes from $p_0L^2/48$ (classical value) for $\lambda = 0$ to 0 for $\lambda \approx 0.2$, while the deflection $w(x)$ remains fixed in its classical form. It may also be useful to explain the reason of such particular behavior.

It is worthy of mention that the characters of the solution of the doubly clamped beam e) are shared by any other Eringen's beam under uniform load p_0, but constrained in such way that *the bending moment is not involved within the boundary conditions (i.e. the rotation is assigned at*

[4] In (Barretta et al., 2018) the numerical/graphical solutions for $\alpha_B = 0.1$ are not reported, but we have been able to obtain these solutions using the closed-form solutions offered by the mentioned authors, except in the case of the clamped-pinned beam d) for which the closed-form solution is not reported.

both beam ends. The latter particular set of beams includes, beside the beam of case e) (for which $w(0) = w(L) = w'(0) = w'(L) = 0$), at least another analogous beam with the boundary conditions $w(0) = w'(0) = w'(L) = 0, M'(L)$ specified.

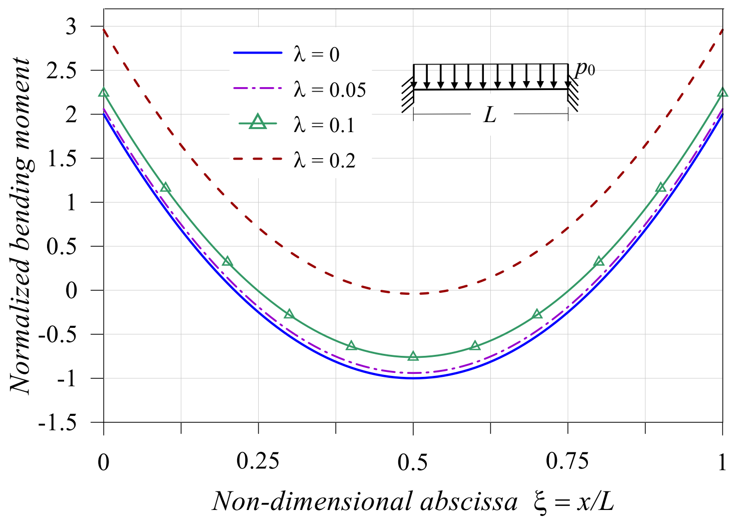

Figure 3: Clamped-clamped Eringen's nonlocal beam under uniform distributed load p_0. Bending moment diagrams $M(x), 0 \leq x \leq L$, reported for different values of $\lambda = 0, 0.5, 0.1, 0.2$.

Then, considering a beam belonging to this particular set, the general governing differential equation, that is,

$$w''''(x) = \frac{1}{EI}\left[p(x) - \ell^2 p''(x)\right] \tag{62}$$

since $p = p_0$, simplifies by losing its dependence on ℓ, namely

$$w''''(x) = \frac{1}{EI} p_0 \tag{63}$$

whereas the bending moment is given by

$$M(x) = -EIw''(x) - \ell^2 p_0 \tag{64}$$

Since the bending moment $M(x)$ does not intervene into the (ordinary) boundary conditions (but its derivative $M'(x)$ possibly does), then the deflection $w(x)$ obtained by integration of (63) does not contain ℓ, hence it coincides with the classical deflection; moreover, the bending moment $M^c(x) := -EIw''(x)$ is the classical bending moment. Therefore the actual bending moment $M(x)$ is expressed as

$$M(x) = M^c(x) - \ell^2 p_0 \tag{65}$$

That is, $M(x)$ is coincident with $M^c(x)$, but shifted by $\ell^2 p_0$ upward, the more, the larger is ℓ, as shown in Figure 3.

An equivalent explanation based on the analogy proposed by (Barretta and Marotti de Sciarra, 2015) may also be given, but we have preferred the use of direct arguments.

5.3. Description and discussion of the obtained results

The obtained results are illustrated in Figures 4–8, where the maximum beam deflection (here called "normalized deflection", denoted with the symbol $\hat{w}$) is plotted as a function of $\lambda := \ell/L$ varying within the (meaningful) interval $(0 \le \lambda \le 0.2)$.

Figures 4–8 show that —except the Eringen's nonlocal method— the other three methods (hereafter collectively referred as the "comparison methods") predict stiffening size effects for all the considered beam cases. The curves $\hat{w}(\lambda)$ obtained with these comparison methods for every beam case are generally sufficiently close to one another, which means that the size effects predictions by the considered methods are in substantial agreement with one another.

The normalized deflection curves, $\hat{w}(\lambda)$, are all characterized by a *negative slope*, namely $\frac{\mathrm{d}\hat{w}}{\mathrm{d}\lambda} < 0$. This indicates that there is a *reduction of the normalized deflection with increasing* λ, or equivalently that there is an *increase of the stiffening effects with decreasing the specimen size.* This result is a natural consequence of the physical circumstance whereby the microstructure with its stiffening effects becomes dominant the more, the smaller is the specimen size.

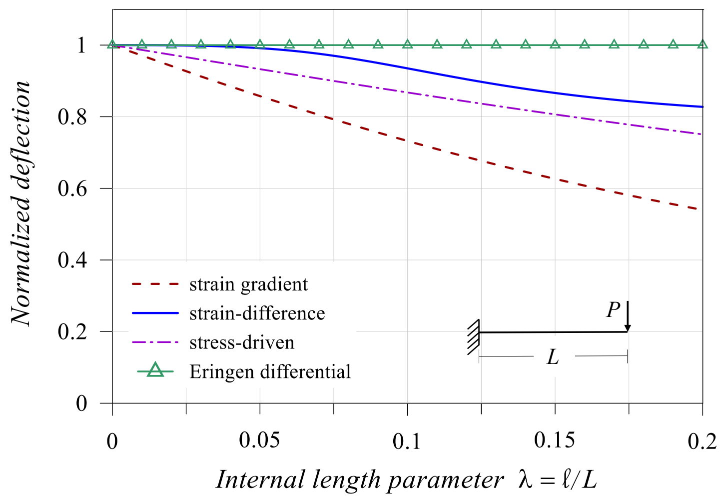

Figure 4: Cantilever beam subjected to a point load at the free end. Normalized deflection at the free end cross section *versus* internal length parameter λ for strain gradient (Polizzotto 2014, dashed line), strain-difference integral (present model, solid line), stress-driven (Barretta et al. 2018, dash dot line) and Eringen differential (Peddieson et al. 2003, solid line with triangles) constitutive behavior.

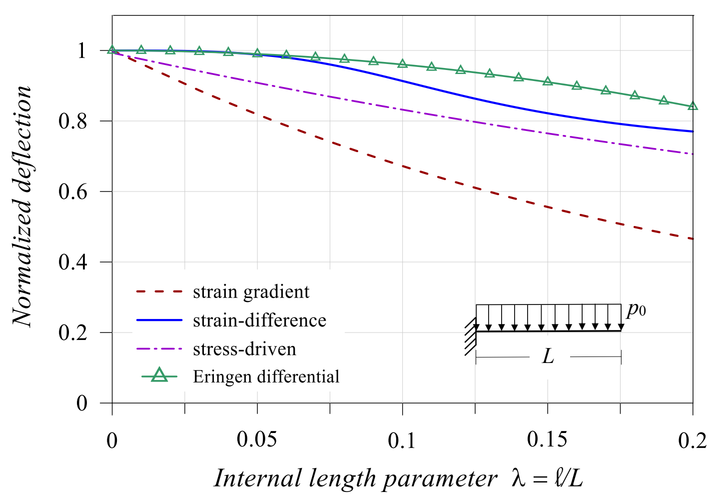

Figure 5: Cantilever beam subjected to uniform distributed load. Normalized deflection at the free end cross section *versus* internal length parameter λ for strain gradient (Polizzotto 2014, dashed line), strain-difference integral (present model, solid line), stress-driven (Barretta et al. 2018, dash dot line) and Eringen differential (Peddieson et al. 2003, solid line with triangles) constitutive behavior.

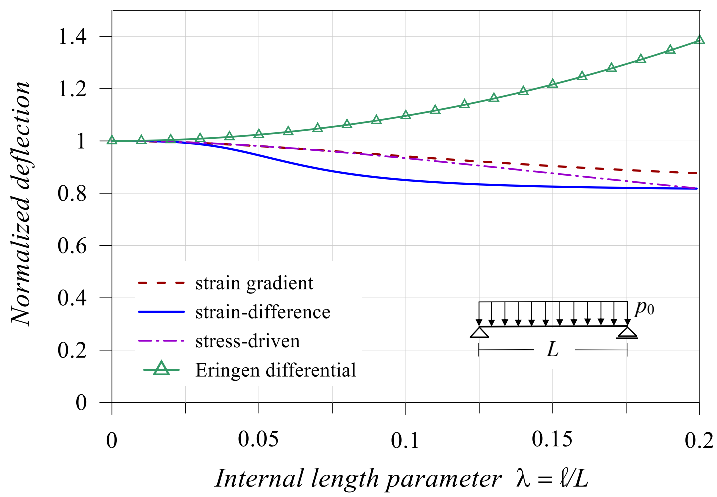

Figure 6: Simply supported beam subjected to uniform distributed load. Normalized deflection at mid cross section *versus* internal length parameter for strain gradient (Polizzotto 2014, dashed line), strain-difference integral (present model, solid line), stress-driven (Barretta et al. 2018, dash dot line) and Eringen differential (Peddieson et al. 2003, solid line with triangles) constitutive behavior.

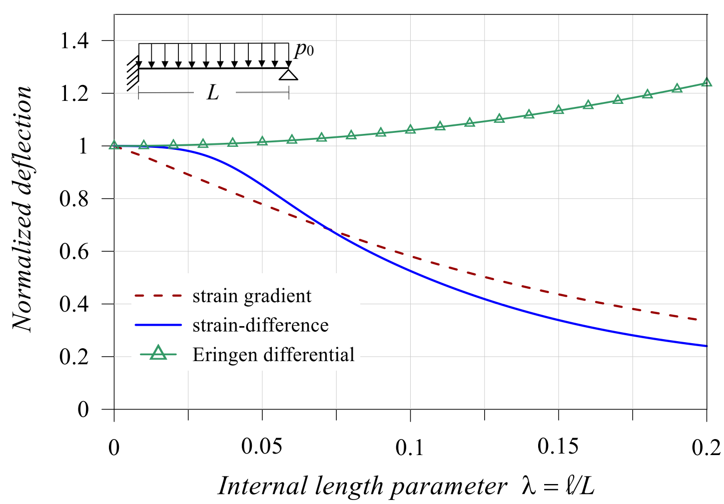

Figure 7: Clamped-pinned beam subjected to uniform distributed load. Normalized deflection at mid cross section *versus* internal length parameter λ for strain gradient (Polizzotto 2014, dashed line), strain-difference integral (present model, solid line) and Eringen differential (Peddieson et al. 2003, solid line with triangles) constitutive behavior. (The curve relative to the stress-driven model is not reported because the related closed-form solution is not reported in (Barretta et al., 2018).)

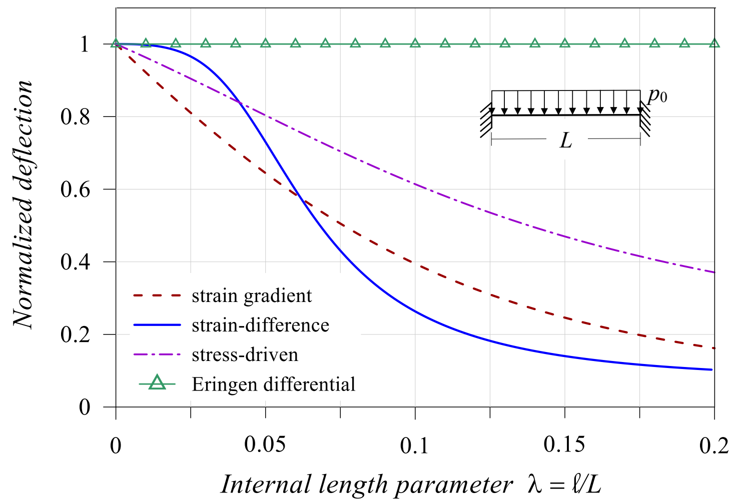

Figure 8: Clamped-clamped beam subjected to uniform distributed load. Normalized deflection at mid cross section *versus* internal length parameter λ for strain gradient (Polizzotto 2014, dashed line), strain-difference integral (present model, solid line), stress-driven (Barretta et al. 2018, dash dot line) and Eringen differential (Peddieson et al. 2003, solid line with triangles) constitutive behavior.

Figures 4–8 show that the normalized deflection curves relative to the strain-difference based model exhibit a waved pattern. This means that, after the latter model, the rate at which the stiffening effects increase is increasing with λ increasing from zero to some inflection point, say λ^i, but is decreasing with λ increasing beyond λ^i. This prediction of the strain-difference based model seems to be in contrast with the strain gradient model and the stress-driven one, which in fact lead to normalized deflection curves that apparently do not exhibit a waved pattern.

However, a deeper insight on Figures 4–8 shows that both the strain gradient model and the stress-driven one may also lead to waved curves $\hat{w}(\lambda)$, though with less pronounced wave amplitudes, for certain beam cases. This has been ascertained by computing the slope $\mathrm{d}\hat{w}/\mathrm{d}\lambda$ as a function of λ. We found a waved normalized deflection curve for the doubly pinned beam case addressed with either the strain-gradient and the stress-driven models, as well as for the clamped-pinned and doubly clamped beam cases addressed with the stress-driven model.

For a full validation of the above waved pattern of the normalized deflection suitable experimental data would be required, but —to the authors' knowledge— such data are not available. In the wait of the necessary (likely difficult) laboratory experiments, the existence of normalized deflection curves with a waved pattern remain as just a prediction of the existing constitutive models.

6. Conclusion

We have applied the so-called strain-difference based nonlocal elasticity model previously devised elsewhere (Polizzotto et al., 2004, 2006) to simple Euler-Bernoulli beam structures subjected to static loads. Stiffening size effects have been found for the five beam cases herein considered, while the proposed method is expected to lead to the same kind of size effects for other types multi-dimensional structures. For comparison, the beam responses based on other constitutive models have been also reported, namely, the strain gradient model (Mindlin and Eshel, 1968; Papargyri-Beskou et al., 2003a,a; Polizzotto, 2014), along with the stress-driven nonlocal model (Romano and Barretta, 2017a,b; Romano et al., 2017b). Stiffening size effects were also found with these latter models. The comparison was enriched by reporting the analogous plots obtained with the Eringen nonlocal differential model, known to lead to inconsistent solutions (paradoxes).

The major notable result obtained with the present work is that stiffening size effects on the deformation for the five considered beam cases (and likely for other multi-dimensional structures) are predicted with the proposed strain-difference based nonlocal model, which belongs to the family of strain-integral nonlocal models.

The obtained results prove to be in sufficient agreement with those obtained with the widely accepted strain-gradient constitutive model, as well as with the stress-driven model by Romano and Barretta (2017a,b), which seems to corroborate the well-known *smaller-is-stiffer* phenomenon. For a full validation of these results, arguments based on adequate laboratory experiments would be required. Due to the difficulty to find out adequate experimental data, here a theoretical study has been performed.

In the authors' opinion, the obtained results deserve to be further pursued, first in order to find improved models to adhere more accurately to the actual (experimentally validated) specimen behavior, second in order to extend the application framework. This is the subject of an ongoing research.

References

Abazari A.M., Safavi S.M., Rezazadeh G., Villanueva L.G., 2015. Modelling the size effects on the mechanical properties of micro/nano structures. Sensors 15, 28543–28562.

Aydogdu M., 2009. A general nonlocal beam theory: Its application to nanobeam bending, buckling and vibration. Physica E 41, 1651–1655.

Barretta R., Marotti de Sciarra F., 2015. Analogies between nonlocal and local Bernoulli–Euler nanobeams. Arch. Appl. Mech. 85, 89–99.

Barretta R., Fabbroncino F., Luciano R., Marotti de Sciarra F., 2018. Closed-form solutions in stress-driven two-phase integral elasticity for bending of functionally graded nono-beams. Physica E 97, 13–30.

Benvenuti E., Simone A., 2013. One-dimensional nonlocal and gradient elasticity: Closed-form solution and size effects. Mech. Res. Commun. 48, 46–51.

Borino G., Failla B., Parrinello F., 2002. A symmetric formulation for nonlocal damage models. In: Mang H.A., Rammerstoffer F.G., Eberhardsteiner J., (Eds), Proc. 5th Congress on Computational Mechanics (WCCM V), University of Technology, Wien.

Borino G., Failla B., Parrinello F., 2003. A symmetric nonlocal damage theory. Int. J. Solids Struct. 40, 3621–3645.

Challamel N., Wang C.M., 2008. The small length scale effect for a non-local cantilever beam: A paradox solved. Nanotechnology 19(34), 345703.

Challamel N., Reddy J.N., Wang C.M., 2016. Eringen's stress gradient model for bending of nonlocal beams. J. Eng. Mech. 142, 10.1061/(ASCE)EM.1943-7889-0001161.

Eltaher M.A., Khater M.E., Emam S.A., 2016. A review on nonlocal elastic models for bending, buckling, vibrations and wave propagation of nanoscale beams. Appl. Math. Modelling 40, 4109–4128.

Eptaimeros K.G., Koutsoumaris C.Chr., Tsamasphyros G.J., 2016. Nonlocal integral approach to the dynamical response of nanobeams. Int. J. Mech. Sci. 115-116, 68–80.

Eringen, A.C., 1972. Linear theory of nonlocal elasticity and dispersion of plane waves. Int. J. Eng. Sci. 10(5), 425–435.

Eringen A.C., 1983. On differential equations of nonlocal elasticity and solutions of screw dislocation and surface waves, J. Appl. Phys. 54, 4703–4710.

Eringen A.C., 1987. Theory of nonlocal elasticity and some applications. Res Mech. 21, 313–342.

Eringen A.C., 2002. Nonlocal Continuum Field Theories, Springer-Verlag, New York.

Faroughi Sh., Goushegir S.M.H., Haddad Khodaparast H., Friswell M.I., 2017. Nonlocal elasticity in plates using novel trial functions. Int. J. Mech. Sci. 130, 221–233.

Fernández-Sáez J., Zaera R., Loya J.A., Reddy J.N., 2016. Bending of Euler–Bernoulli beams using Eringen's integral formulation: A paradox solved. Int. J. Eng. Sci. 99, 107–116.

Fleck N.A., Muller G.M., Ashby M.F., Hutchinson J.W., 1994. Strain gradient plasticity: Theory and experiments. Acta Metallurgica et Materialia 42, 475–487.

Gao, X.-L., Park, S.K., 2007. Variational formulation of a simplified strain gradient elasticity theory and its application to pressurized thick-walled cylinder problem, Int. J. Solids Struct. 44, 7486–7499.

Gibson R.F., Ayorinde E.O., Wen Y.-F., 2007. Vibrations of carbon nanotubes and their composites: A review, Composite Science and Technology 67, 1–28.

Heireche H., Tounsi A., Benzair A., Maachou M., Adda Bedia E.A., 2008. Sound wave propagation in single-walled carbon nanotubes using nonlocal elasticity, Physica E 40, 2791–2799.

Khodabakhshi P., Reddy J.N., 2015. A unified integro-differential nonlocal model. Int. J. Eng. Sci. 95, 60–75.

Khorshidi K., Fallah A., 2016. Buckling analysis of functionally graded rectangular nano-plate based on nonlocal exponential shear deformation theory. Int. J. Mech. Sci. 113, 94–104.

Kumar D., Heinrich C., Waas A.M., 2008. Buckling analysis of carbon nanotubes modeled using nonlocal continuum theories, J. Appl. Phys. 103, 073521.

Lam D.C.C., Yang F., Chong A.C.M., Wang J., Tong P., 2003. Experiments and theory in strain gradient elasticity. J. Mech. Phys. Solids 51, 1477–1508.

Li C., Yao L., Chen W., Li S., 2015. Comments on nonlocal effects in nanocantilever beams. Int. J. Eng. Sci. 87, 47–57.

Li Z., He Y., Lei J., Guo S., Liu D., Wang L., 2018. A standard experimental method for determining the material length scale based on modified couple stress theory. Int. J. Mech. Sci. 141, 198–205.

Lim C.W., Zhang G., Reddy J.N., 2015. A higher-order nonlocal elasticity and strain gradient theory and its applications in wave propagation. J. Mech. Phys. Solids 78, 298–313.

Lu P., Lee H.P., Lu C., Zhang P.Q., 2006. Dynamic properties of flexural beams using a nonlocal elasticity model. J. Appl. Phys. 99, 1–9.

Lu L., Guo X., Zhao J., 2017. Size-dependent vibration analysis of nanobeams based on the nonlocal strain gradient theory. Int. J. Eng. Sci. 116, 12–24.

Mindlin R.D., 1965. Second gradient of strain and surface-tension in linear elasticity. Int. J. Solids Struct. 1, 417–438.

Mindlin R.D., Eshel N.N., 1968. On first strain-gradient theories in linear elasticity, Int. J. Solids Struct. 4, 109–124.

Pang M., Li Z.L., Zhang Y.Q., 2018. Size-dependent transverse vibration of viscoelastic nanoplates including high-order surface stress effect. Phisica B: Condensed Matter 545, 94–98.

Papargyri-Beskou S., Tsepoura K.G., Polyzos D., Beskos D.E., 2003a. Bending and stability analysis of gradient elastic beams. Int. J. Solids Struct. 40 (2), 385–400.

Papargyri-Beskou S., Tsepoura K.G., Polyzos D., Beskos D.E., 2003b. Dynamic analysis of gradient elastic flexure beams. Struct. Engng. and Mechs. 15 (6), 705–716.

Patra A.K., Gopalakrishnan S., Ganguli R., 2018. Unified nonlocal rational continuum models developed from discrete atomistic equations. Int. J. Mech. Sci. 135, 176–189.

Peddieson J., Buchanan G.R., McNitt R.P., 2003. Application of nonlocal continuum models to nanotechnology. Int. J. Eng. Sci. 41, 305–312.

Pijaudier-Cabot G., Bažant Z.P., 1987. Nonlocal damage theory. J. Engng. Mech. ASCE 113, 1512–1533.

Pin Lu, Zhang P.Q., Lee H.P., Wang C.M., Reddy J.N., 2007. Nonlocal elastic plate theories. Proc. R. Soc. A 463, 3225–3240.

Pinto Y., Mordehai D., 2018. Size-dependent coupled longitudinal-transverse vibration of five-fold twinned nanowires. Extreme Mechanics Letters 23, 49–54.

Pisano A.A., Fuschi P., 2003. Closed form solution for a nonlocal elastic bar in tension. Int. J. Solids Struct. 40, 13–23.

Polizzotto, C., 2001. Nonlocal elasticity and related variational principles. Int. J. Solids Struct. 38, 7359–7380.

Polizzotto C., 2002. Remarks on some aspects of nonlocal theories of solid mechanics. In: Proc. 6th Congress of the Italian Society for Applied and Industrial Mathematics (SIMAI), Cagliari, Italy.

Polizzotto C., 2007. Strain-gradient elastic-plastic material models and assessment of the higher order boundary conditions. Eur. J. Mech. A/Solids 26, 189–211.

Polizzotto C., 2014. Stress gradient versus strain gradient constitutive models within elasticity. Int. J. Solids Struct. 51, 1809–1818.

Polizzotto C., 2015. From the Euler–Bernoulli beam to the Timoshenko one through a sequence of Reddy-type shear deformable beam models of increasing order. Eur. J. Mech. A/Solids 53,62–64.

Polizzotto C., 2017. A class of shear deformable isotropic elastic plates with parametrically variable warping shapes. ZAMM-Z. Angew. Math. Mech. 1–27 (2017)/DOI 10.1002/zamm.201700070

Polizzotto C., Fuschi P., Pisano A.A., 2004. A strain-difference-based nonlocal elasticity model. Int. J. Solids Struct. 41, 2383–2401.

Polizzotto C., Fuschi P., Pisano A.A., 2006. A nonhomogeneous nonlocal elasticity model. Eur. J. Mech. A/Solids 25, 308–333.

Polizzotto C., Pisano A.A., 2012. An energy residual-based approach to gradient effects within the mechanics of generalized continua. J. of Mechanical Behavior of Materials 21 (3-4), 101–121.

Polyanin A., Manzhirov A., 2008. Handbook of Integral Equations. CRC Press, New York.

Press W.H., Teukolsky S.A., Vetterling W.T., Flannery B.P., 1997. Numerical Recipes in Fortran 77: The Art of Scientific Computing, Second Edition, Cambridge University Press, NY.

Rafii-Tabar H., Ghavanloo E., Fazelzadeh S.A., 2016. Nonlocal continuum-based modeling of mechanical characteristics of nanoscopic structures. Physics Reports 638, 1–97.

Reddy J.N., 2007. Nonlocal theories for bending, buckling and vibration of beams, Int. J. Eng. Sci. 45, 288–307.

Reddy J.N., 2010. Nonlocal nonlinear formulations for bending of classical and shear deformation theories of beams and plates. Int. J. Eng. Sci. 48(11), 1507–1518.

Romano G. Barretta R., 2016. Comment on the paper "Exact solution of Eringen's nonlocal integral model for bending of Euler–Bernoulli and Timoshenko beams" by Meral Tuna and Mesut Kirca. International Journal of Engineering Science, 109, 240–242.

Romamo G., Barretta R., Diaco M., Marotti de Sciarra F., 2017a. Constitutive boundary conditions and paradoxes in nonlocal elastic nanobeams. Int. J. Mech. Sci. 121, 151–156.

Romano G., Barretta R., 2017a. Nonlocal elasticity in nanobeams: The stress-driven integral model. Int. J. Eng. Sci. 115, 14–27.

Romano G., Barretta R., 2017b. Stress-driven versus strain-driven nonlocal integral model for elastic nano-beams. Composites Part B 114, 184–188.

Romano G., Barretta R., Diaco M., 2017b. On nonlocal integral models for elastic nano-beams. Int. J. Mech. Sci. 131-132, 490–499.

Romano G., Luciano R., Barretta R, Diaco M., 2018. Nonlocal integral elasticity in nanostructures, mixtures, boundary effects and limit behaviours. Continuum Mech, Thermodyn. 30, 641–655.

Sahmani S., Aghdam M.M., Rabczuk T., 2018a. Nonlinear bending of functionally graded porous micro/nano-beams reinforced with graphene platelets based upon nonlocal strain gradient theory. Composite Structures 186, 68–78.

Sahmani S., Aghdam M.M., Rabczuk T., 2018b. Nonlocal strain gradient plate model for nonlinear large-amplitude vibrations of functionally graded porous micro/nano-plates reinforced with GPLs. Composite Structures 198, 51–62.

Sahmani S., Aghdam M.M., Rabczuk T., 2018c. A unified nonlocal strain gradient plate model for nonlinear axial instability of functionally graded porous micro/nano-plates reinforced with graphene platelets. Material Research Express 5, 045048.

Sahmani S., Aghdam M.M., 2017a. Temperature-dependent nonlocal instability of hybrid FGM exponential shear deformable nanoshells including inperfection sensitivity. Int. J. Mech. Sci. 122, 129–142.

Sahmani S., Aghdam M.M., 2017b. Nonlinear instability of axially loaded functionally graded multilayer graphene platelet-reinforced nanoshells based on nonlocal strain gradient elasicity theory. Int. J. Mech. Sci. 131, 95–106.

Shaat M., Abdelkefi A., 2017. New insights on the applicability of Eringen's nonlocal theory. Int. J. Eng. Sci. 121, 67–75.

Sudak L.J., 2003. Column buckling of multiwalled carbon nanotubes using nonlocal continuum mechanics, J. Appl. Phys. 94(11), 7281–7287.

Sun L., Han R.P.S., Wang J., Lim C.T., 2008. Modeling the size-dependent elastic properties of polymeric nanofibers. Nanotechnology 19, 455706.

Tricomi F. G., 1985. Integral Equations. Dover Books on Mathematics, U.K.

Tuna M., Kirca M., 2016. Exact solution of Eringen's nonlocal integral model for bending of Euler–Bernoulli and Timoshenko beams. Int. J. Eng. Sci. 105, 80–92.

Vila J., Fernández-Sáez J., Zaera R., 2017. Nonlinear continuum models for the dynamic behavior of 1D microstructured solids. Int. J. Solds Struct. 117, 111–122.

Wang L., Hu H., 2005. Flexural wave propagation in single-walled carbon nanotubes, Physical Review B 71, 195412 (7pp).

Wang Q., Arash B., 2014. A review on applications of carbon nanotubes and graphenes as nano-resonator sensors. Comput. Mater. Sci. 82, 350–360.

Wang Y.B., Zhu X.W., Dai H.H., 2016. Exact solutions for static bending of Euler–Bernoulli beams using Eringen's two-phase local/nonlocal model. AIP Advances 6, 085114.

Xu X.-J., Deng Z.-C., Zhang K., Xu W., 2016. Observations of the softening phenomenona in the nonlocal cantilever beams. Composite Structures 145, 43–57.

Xu X.-J., Wang X.-C., Zheng M.-L., Ma Z., 2017a. Bending and buckling of nonlocal strain gradient elastic beams. Compos. Struct. 160, 366–377.

Xu X.-J, Zheng M.-L., Wang X.-C., 2017b. On vibrations of nonlocal rods: Boundary conditions, exact solutions and their asymptotics. Int. J. Eng. Sci. 119, 217–231.

Zhang X., Jiao K., Sharma P., Yakobson B.I., 2006. An atomistic and non-classical continuum field theoretic perspective of elastic interactions between defects (force dipoles) and various symmetries and application to graphene. J. Mech. Phys. Solids 54, 2304–2329 (2006).

Zhao H., Min K., Aluru N.R., 2009. Size and chirality dependent elastic properties of graphene nanoribbons under uniaxial tension. Nano Letters 9(8), 3012–3015.